

Direct Electrochemistry of Catalase Immobilized at Electrochemically Reduced Graphene Oxide Modified Electrode for Amperometric H₂O₂ Biosensor

Shan Wei Ting¹, Arun Prakash Periasamy¹, Shen-Ming Chen^{1,*}, R. Saraswathi²

¹ Department of Chemical Engineering and Biotechnology, National Taipei University of Technology, No.1, Section 3, Chung-Hsiao East Road, Taipei 106, Taiwan (R.O.C).

² Department of Materials Science, School of Chemistry, Madurai Kamaraj University, Madurai 625 021, Tamil nadu, India.

*E-mail: smchen78@ms15.hinet.net

Received: 9 August 2011 / Accepted: 12 September 2011 / Published: 1 October 2011

Electrochemically reduced graphene oxide (ERGO) modified glassy carbon electrode (GCE) surface has been used as a novel immobilization matrix for the oxidoreductase enzyme, catalase (CAT) to explore its direct electrochemistry. In order to attach the CAT molecules firmly to the ERGO modified surface and to enhance the anti-interfering ability of the biosensor a thin layer of nafion (NF) was fabricated above the CAT layer. The as-prepared exfoliated graphene oxide (GO), ERGO, CAT and CAT immobilized ERGO films (NF/CAT/ERGO) were characterized by scanning electron microscopy (SEM), energy-dispersive X-ray (EDX) spectra and atomic force microscopy (AFM) studies. The electrochemical behavior and the interfacial changes occurring at all the modified electrodes were probed via electrochemical impedance spectroscopy (EIS) technique. The fabricated NF/CAT/ERGO film based biosensor exhibits quick response (5 s), excellent electrocatalytic activity towards H₂O₂ in the linear concentration range from 0.05 to 1.91 mM with a sensitivity of 7.76 $\mu\text{A mM}^{-1} \text{cm}^{-2}$. The proposed CAT biosensor also shows high selectivity towards H₂O₂, which opens up its practical applications.

Keywords: Direct electrochemistry, catalase, electrochemically reduced graphene oxide, electrocatalysis, hydrogen peroxide.

1. INTRODUCTION

In the last half decade, graphene is a promising electrode material known for its attractive mechanical, electronic and thermal properties and it has been widely used for the construction of field effective transistors, sensors and other clean energy based devices [1]. In addition, the unique

electrochemical properties of graphene such as excellent conductivity, fast electron transfer, wide electrochemical potential window, ability to enhance the direct electron transfer between the enzymes and the bare electrodes have broadened their applications in the field of electrochemical biosensors [2]. Hitherto, the typical graphene synthesis routes such as micromechanical cleavage of graphite are though advantageous, they failed to produce perfect two-dimensional atomic crystals in large scales and leads to the scrolling and folding at the edges [3]. Alternatively, versatile strategies have been employed by the researchers to achieve large yield, high-electronic quality graphene [4, 5]. Moreover, the graphene sheets prepared by the much preferred chemical exfoliation method are not good enough for nanoelectronics applications [6]. On the other hand, with high sensitivity, low-cost and green approach (without using any toxic solvents), the electrochemical reduction method is more efficient for preparing high quality graphene sheets in large scale in a short time from exfoliated graphene oxide (GO) [7].

Catalase (CAT) is an important enzyme of oxidoreductase family which has been widely employed in biosensors for sensitive and selective H_2O_2 determination [8]. However, the selection of suitable electrode material and novel immobilization matrices with good electronic properties is essential to enhance the direct electron transfer between CAT and the electrode surfaces. Previous studies emphasis the key roles played by the nanomaterials in promoting the direct electrochemistry of CAT [9]. Several nanomaterial modified matrices have been employed by many research groups to study the direct electrochemistry behavior of CAT [10-12]. Recently, Huang *et al.* have reported the direct electrochemistry of CAT at a nanocomposite matrix containing amine-functionalized graphene and gold nanoparticles [13].

In our previous study, we have reported the direct electrochemistry of CAT at nafion (NF) wrapped multiwalled carbon nanotubes (MWCNTs) in the presence of cationic surfactant, didodecyldimethylammonium bromide (DDAB) through electrostatic interactions between CAT, MWCNT-NF and DDAB. Owing to the unique physical and electrochemical properties of graphene, in this study, we have attempted to explore the direct electrochemistry of CAT at electrochemically reduced graphene oxide (ERGO) modified glassy carbon electrode (GCE) surface. We have followed a simple, cost-effective, facile route to reduce GO electrochemically at high negative potential (-1.3 V) vs. Ag/AgCl reference electrode. The fabricated NF/CAT/ERGO modified electrode exhibits excellent electrocatalytic activity towards H_2O_2 in good linear range with acceptable sensitivity and stability.

2. EXPERIMENTAL

2.1. Reagents

Graphite powder was purchased from Sigma-Aldrich. CAT from bovine liver ($4540 \text{ units mg}^{-1}$) was purchased from Sigma. 5 wt% nafion (NF) perfluorinated ion exchange resin was obtained from Aldrich. H_2O_2 (30%) was obtained from Wako pure chemical Industries, Ltd. The supporting electrolyte used in this study is 0.05 M pH 7 phosphate buffer solution (PBS). PBS was prepared using 0.05 M Na_2HPO_4 and NaH_2PO_4 solutions. All the reagents used in this work were of analytical grade and all aqueous solutions were prepared using doubly distilled water. Prior to each experiment, the

experimental solutions were deoxygenated with pre-purified N₂ gas for 10 min and the N₂ tube was kept above the solutions to maintain an inert atmosphere.

2.2. Apparatus

Cyclic voltammetry (CV) experiments were carried out using CHI 1205a work station. A conventional three electrode cell containing freshly prepared 0.05 M PBS (pH 7) was used for electrochemical studies. GCE with an electrode surface area of 0.079 cm² was used as working electrode. Pt wire with 0.5 mm diameter was used as counter electrode and all the potentials were referred with respect to standard Ag/AgCl reference electrode. EIM6ex ZAHNER (Kroanch, Germany) was used for electrochemical impedance spectroscopy (EIS) studies. Surface morphology studies were carried out using Hitachi S-3000 H scanning electron microscope (SEM) and Being nano-instruments CSPM 4000, atomic force microscope (AFM). Energy-dispersive X-ray (EDX) spectra was recorded using HORIBA EMAX X-ACT (Model 51-ADD0009, Sensor + 24V=16 W, resolution at 5.9 keV = 129 eV). Amperometric (i-t curve) measurements were performed using CHI-750 potentiostat with analytical rotator AFMSRX (PINE instruments, USA).

2.3. Graphene oxide (GO) preparation

Graphene oxide was prepared from graphite as per the procedure reported by Staudenmaier [14, 15]. In a typical procedure, about 2.5g of graphite was added to a mixture containing 44 ml of concentrated sulfuric acid and 29 ml of nitric acid in a fume hood. With constant stirring of the graphite mixture, 23 g of potassium chlorate was slowly added to the graphite mixture over 30 min (To avoid any violent or explosive reactions, slow and controlled addition of potassium chlorate is essential). The resulting suspension was stirred for 5 days during which yellowish gas evolved from the mixture and the color of the mixture changed from yellow to blue. The mixture was diluted with 2 L of water, filtered through coarse filter paper and thus obtained filter cake was washed with 250 ml of 5 % HCl solution. The as-prepared graphene oxide was resuspended in water and centrifuged to remove any excess HCl. The washing cycle was repeated few times, remaining solid was dried at 353 K overnight and ground up with a mortar and pestle to a fine powder.

2.4. Fabrication of ERGO modified GCE

In order to exfoliate the GO sheets, 1 mg of GO was dispersed in 1 ml of double distilled water and the whole solution was ultrasonicated for 1 h. GCE surface was polished to a mirror finish on a clean Buehler polishing cloth using 0.05 μm alumina slurry. In order to remove the loosely adsorbed alumina particles the polished GCE surface was washed and ultrasonicated in doubly distilled water for 10 min. 10 μl of GO dispersion was drop casted on the clean GCE surface and dried at room temperature for 2 h. After 2 h, thus obtained GO modified GCE was gently washed with doubly distilled water and then transferred to an electrochemical cell containing 0.05 M PBS (pH 5). As

shown in Fig. 1, 15 consecutive cyclic voltammograms were performed in the potential range between 0 and -1.5 V at the scan rate of 50 mV s^{-1} .

In Fig. 1, during the first cycle scan a large cathodic peak appears at -1.3 V with a starting potential of -0.75 V. As reported by Guo *et al.* the appearance of enhanced reduction peak with large reduction current can be attributed to the reduction of surface oxygen groups [6]. However, from the second cycle onwards the reduction current observed at negative potentials decreases notably and disappears after several potential scans. This validates the quick and irreversible reduction of surface-oxygenated species of GO at negative potentials and the advantage of electrochemical approach to reduce the exfoliated GO.

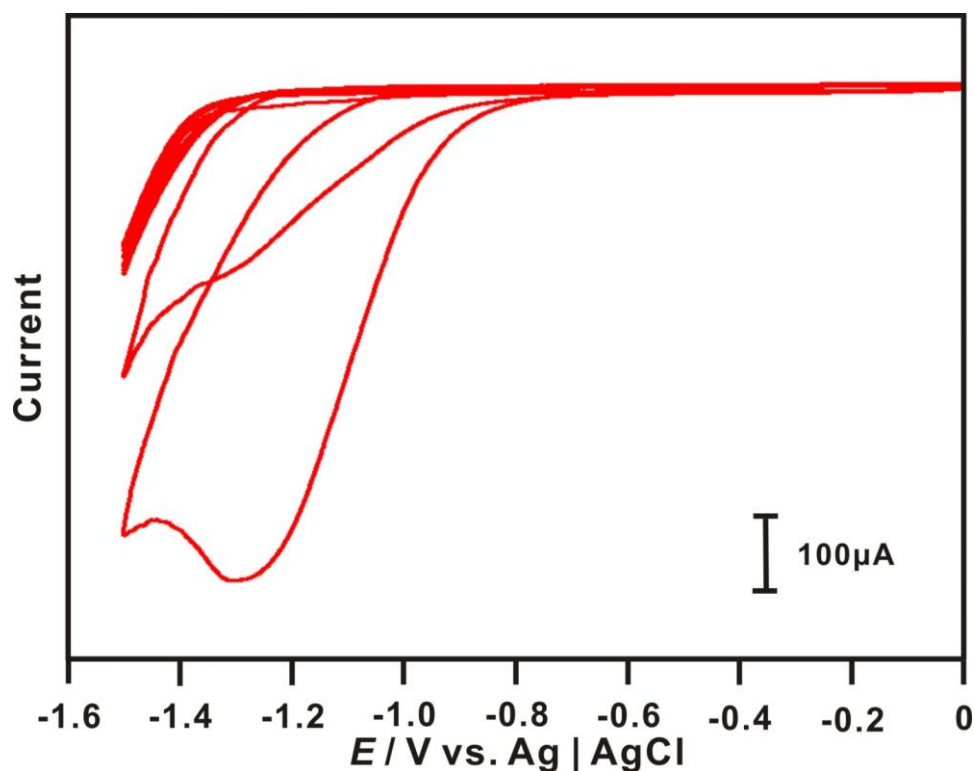


Figure 1. 15 consecutive cyclic voltammograms recorded at a GO modified GCE in N_2 saturated 0.05 M PBS (pH 5.0) at the scan rate of 50 mV s^{-1} .

2.5. Immobilization of CAT at ERGO modified GCE

10 mg ml^{-1} of CAT solution was prepared in 0.05 M PBS (pH 7). Similarly, 0.5 % NF solution was prepared in ethanol. The ERGO modified GCE was utilized for CAT immobilization. About $10 \mu\text{l}$ of CAT solution was drop casted on the ERGO modified GCE surface and dried at 25°C for 1 h. The CAT modified surface was gently washed with doubly distilled water and dried. Finally to hold the CAT molecules firmly at the ERGO surface and to avoid leaching of the CAT molecules, $2 \mu\text{l}$ of 0.5 % NF solution was drop casted and dried at 25°C for half an hour. Finally, the fabricated NF/CAT/ERGO film modified GCE surface was washed with doubly distilled water and used for

further studies. For comparison, ERGO and CAT modified GCEs were also prepared. All the modified electrodes were stored in 0.05 M PBS (pH 7) at 4°C when not in use.

3. RESULTS & DISCUSSIONS

3.1. Direct electrochemistry of CAT

The electrochemical behavior of various modified electrodes has been investigated in N₂ saturated 0.05 M PBS (pH 7) using CV. The cyclic voltammograms were recorded at ERGO, CAT and NF/CAT/ERGO modified GCEs in the potential range from 0.1 to -0.8 V.

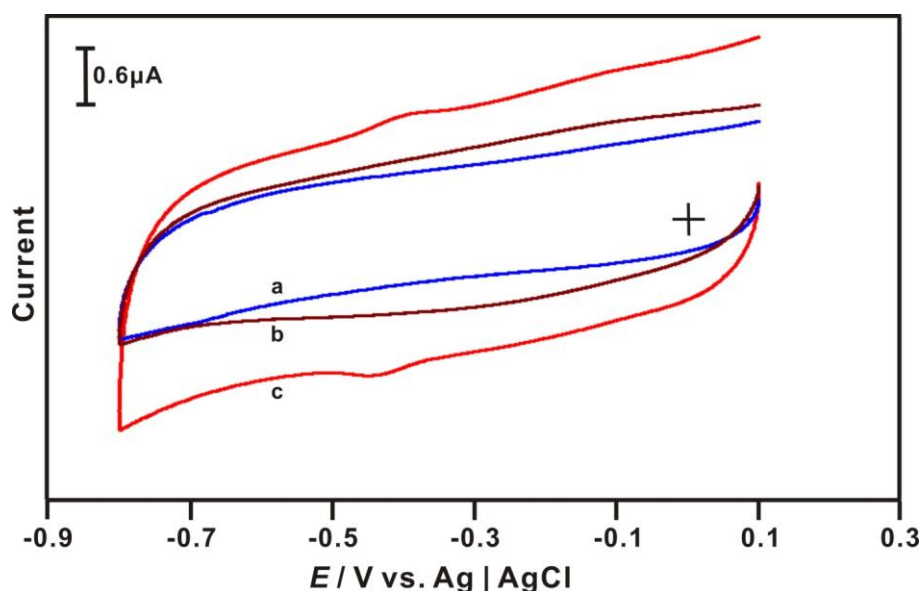


Figure 2. Cyclic voltammograms obtained at (a) ERGO, (b) CAT and (c) NF/CAT/ERGO film modified GCEs in N₂ saturated 0.05 M PBS (pH 7) at the scan rate of 50 mV s⁻¹.

As can be seen from Fig. 2, no redox peaks were observed at both ERGO and CAT film modified GCEs in the above mentioned potential range. However, in the same potential window NF/CAT/ERGO film modified GCE exhibits well defined quasi reversible redox peaks at a formal potential (E°) of -0.41 V. The redox peaks can be attributed to the Fe^{III/II} redox process of CAT, validating the direct electron transfer between CAT and the ERGO modified GCE. The direct electron transfer process occurring at the composite film surface is due to the good electrical communication established with the redox centre of CAT by ERGO.

3.2. Different scan rate studies

Fig. 3 shows the cyclic voltammograms obtained at NF/CAT/ERGO/GCE in N₂ saturated 0.05 M PBS (pH 7) at different scan rates. The peak currents (I_{pa} and I_{pc}) vs. scan rates plot shown in Fig. 3 inset exhibits a linear relationship with $R^2 = 0.997$ and 0.9965 , respectively. Both I_{pa} and I_{pc} increased

linearly with increase in scan rates between 50–2000 mV s^{-1} , thus the redox process occurring at NF/CAT/ERGO/GCE is surface-confined.

The surface coverage (Γ) value of CAT immobilized at NF/CAT/ERGO/GCE has been calculated using the formula given in equation (1)

$$\Gamma = Q/nFA \quad (1)$$

Where, Q is the charge, n is the number of electrons transferred, F is the Faraday current and A is the electrode area. Where, the number of electrons transferred is 1 for $\text{Fe}^{\text{III/II}}$ redox reaction of CAT. The Γ value of CAT immobilized at NF/CAT/ERGO/GCE is calculated to be about $9.51 \times 10^{-12} \text{ mol cm}^{-2}$, indicating monolayer of CAT immobilized at the ERGO surface.

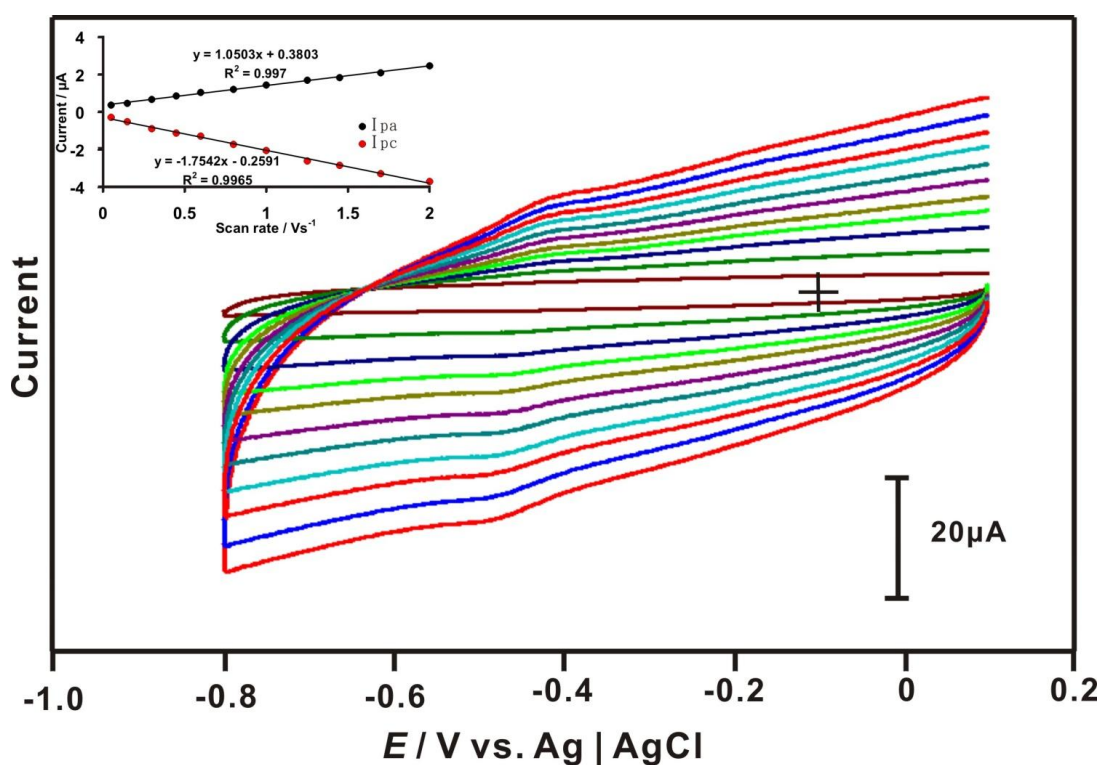


Figure 3. CVs recorded at NF/CAT/ERGO/GCE in N_2 saturated 0.05 M PBS (pH 7) at different scan rates. The scan rates are from inner to outer are 50, 150, 300, 450, 600, 800, 1000, 1250, 1450, 1700 and 2000 mV s^{-1} , respectively. Inset shows the linear dependence of I_{pa} & I_{pc} on scan rate.

3.3. Effect of pH

As shown in Fig. 4, well-defined quasi-reversible redox peaks corresponding to $\text{Fe}^{\text{III/II}}$ redox process of CAT was observed at NF/CAT/ERGO/GCE in the pH range between 1 and 11. The anodic peak currents increased with increase in pH of the solution. However, no obvious redox peaks were observed in pH 13, attributed to the loss of enzyme activity at higher pH [8]. As shown in Fig. 4 inset, the $E^{\circ'}$ of the $\text{Fe}^{\text{III/II}}$ redox couple of CAT exhibits linear dependence on pH of the solution. The $E^{\circ'}$ values showed a negative shift with increase in pH with a slope value of 50.5 mV pH^{-1} . This slope

value is close to the theoretical slope value of 59 mV pH^{-1} for equal number of electron and proton transfer process.

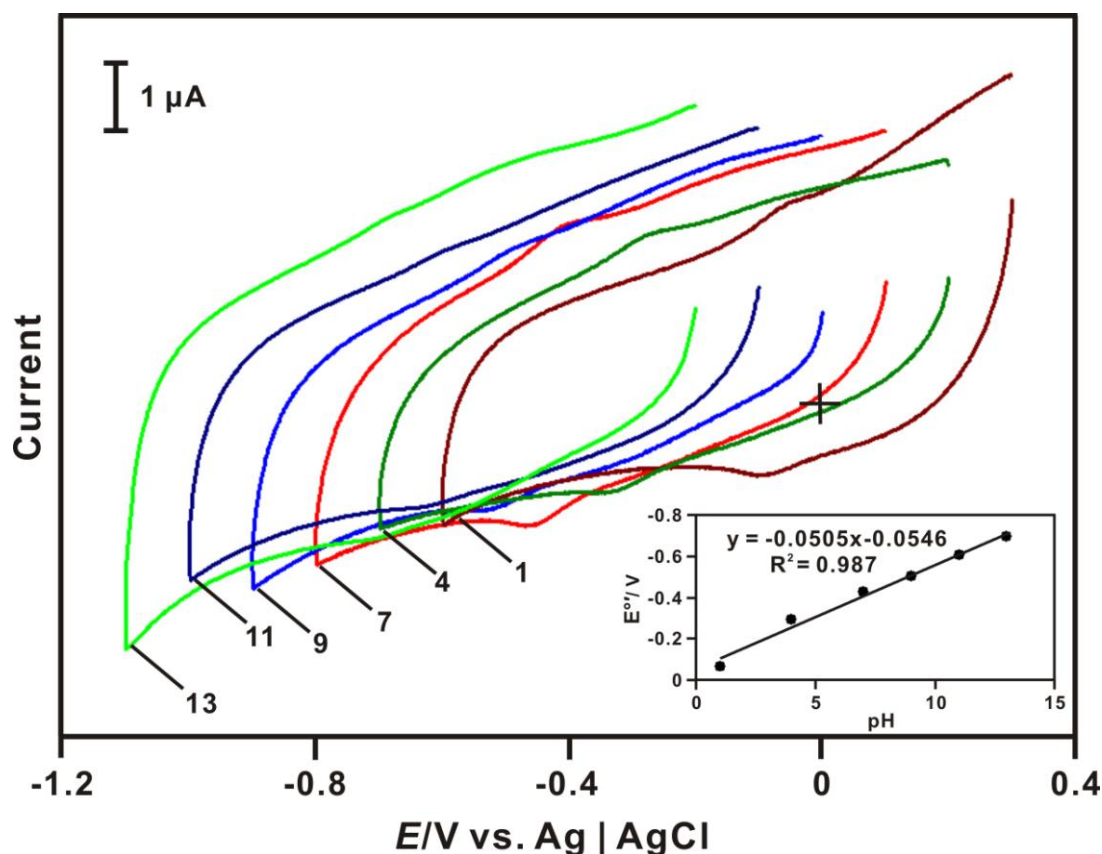


Figure 4. The effect of pH on the redox behavior of NF/CAT/ERGO/GCE in various buffer solutions with pH: 1, 4, 7, 9, 11 and 13, respectively. The inset is E° vs. pH plot.

3.4. SEM, EDX and AFM studies

The surface morphology of various films has been investigated using SEM studies. Fig. 5 (a) and (a') shows the SEM images of CAT film obtained at low and high magnifications. The CAT film surface possesses randomly distributed bright bud like structures, validating the poor immobilization of CAT at bare electrode surface. Whereas, Fig. 5 (b) and (b') shows the SEM image of GO sheets obtained at low and high magnifications. The GO film surface displays fine folded sheets. However, few un-exfoliated GO has also been observed. In contrast, Fig. 5 (c) and (c') displays the SEM images of ERGO sheets with several fine folding and paper like surface morphology, validating the efficient reduction of GO. From the SEM images of NF/CAT/ERGO films shown in Fig. 5 (d) and (d'), it is clear that bud like structures of CAT have been uniformly distributed above the ERGO sheets. Moreover, the typical surface morphology of ERGO sheets such as fine folding has also been observed here. SEM results thus confirmed the efficient immobilization of CAT at the ERGO surface.

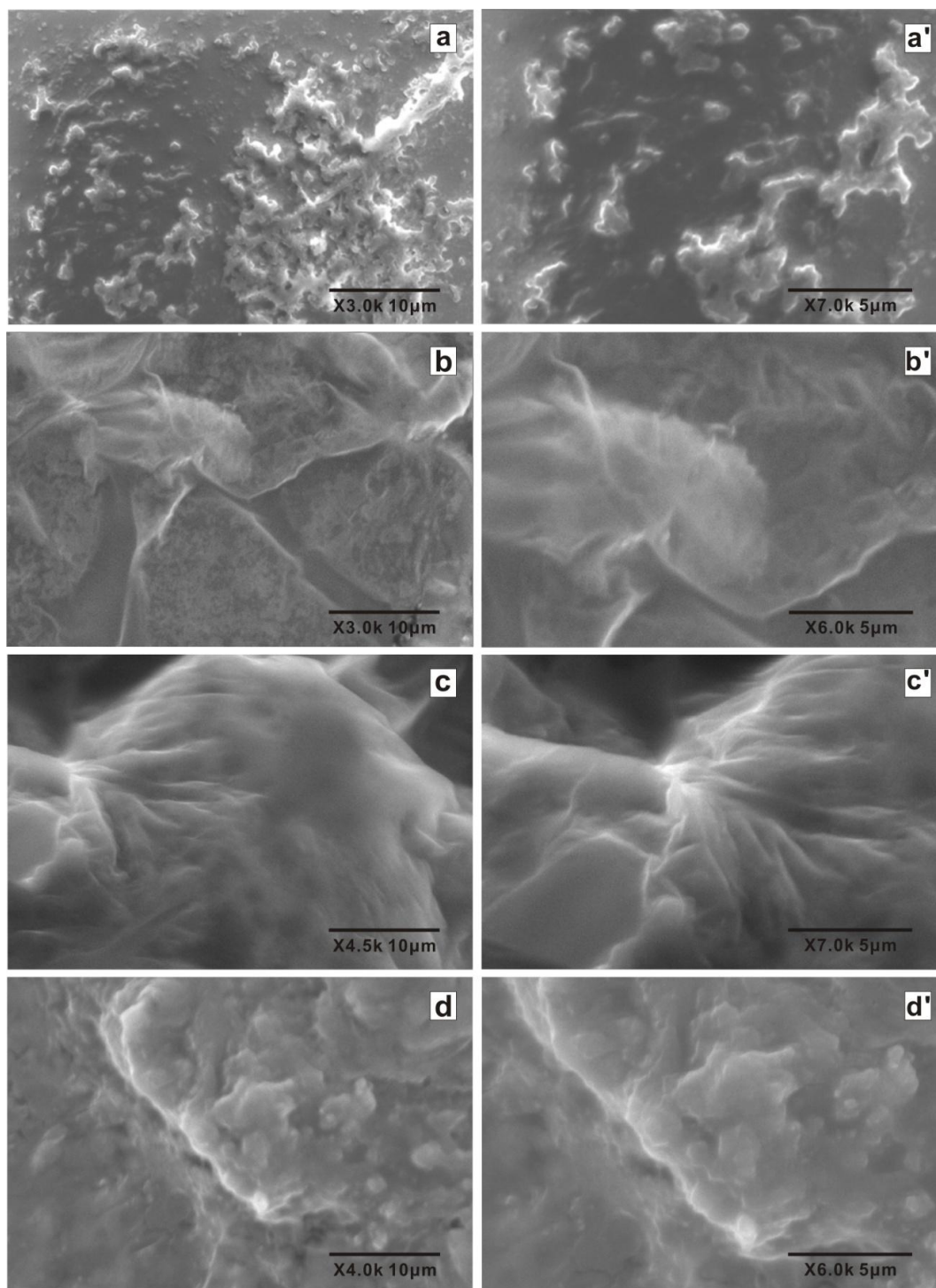


Figure 5. SEM images of CAT (a-a'), GO (b-b'), ERGO (c-c'), and NF/CAT/ERGO (d-d') films at different magnifications.

EDX spectra studies have been carried out at ERGO and NF/CAT/ERGO films to confirm the presence of C and O elements and the purity of ERGO sheets. As shown in Fig. 6 (A), the quantitative results obtained from the EDX spectra of ERGO film contains 48.58 % of C and 51.42 % of O elements, indicating the purity and adequate C and O content in the as-prepared ERGO. Similarly, the quantitative results obtained from the EDX spectra of NF/CAT/ERGO film represents that 50.78 % of

C and 49.22 % of O are present in the composite film (See Fig. 6 (B)). The adequate amount of C and O content in the composite film indicates the presence of sufficient amount of ERGO.

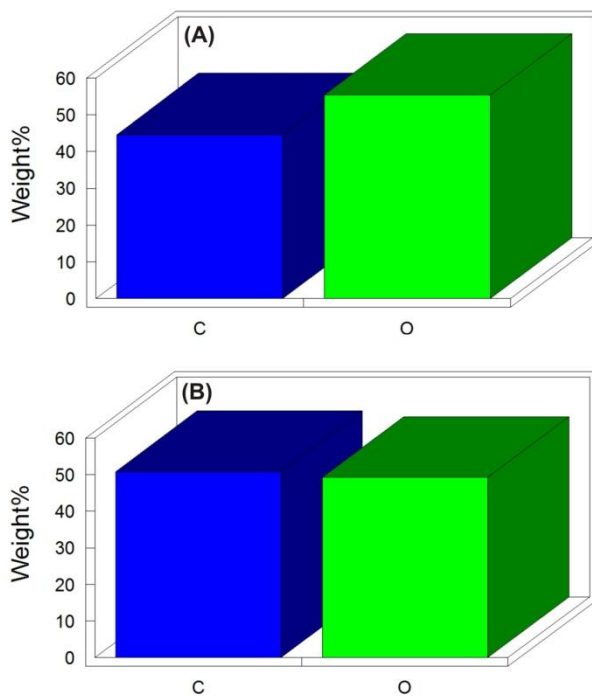


Figure 6. Quantitative results obtained from the EDX spectra of (A) ERGO and (B) NF/CAT/ERGO films.

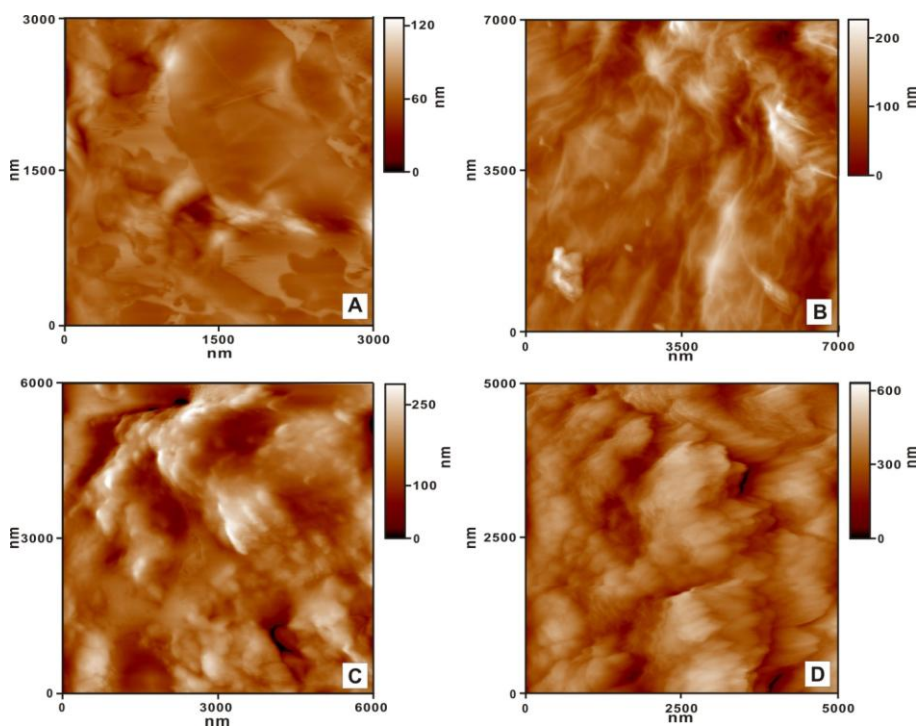


Figure 7. AFM images of (A) GO, (B) ERGO, (C) CAT and (D) NF/CAT/ERGO films.

Fig. 7 (A) shows the AFM image of GO film having plain sheet like surface morphology. Small bright particles and fine folding are also found on the GO film surface. On the other hand, AFM image of ERGO shown in Fig. 7 (B) displays crushed fabric like surface morphology with numerous folding. However, individual ERGO sheets are not found here. Fig. 7 (C) shows CAT film surface containing bright, globular beads. Fig.7 (D) shows the CAT immobilized ERGO film surface. More bud like CAT molecules are uniformly loaded throughout the ERGO surface. AFM results are in good accordance with the SEM results and they ultimately confirmed that CAT has been efficiently immobilized at the ERGO surface.

3.5. Investigation of electrochemical behavior of various film modified electrodes using EIS studies

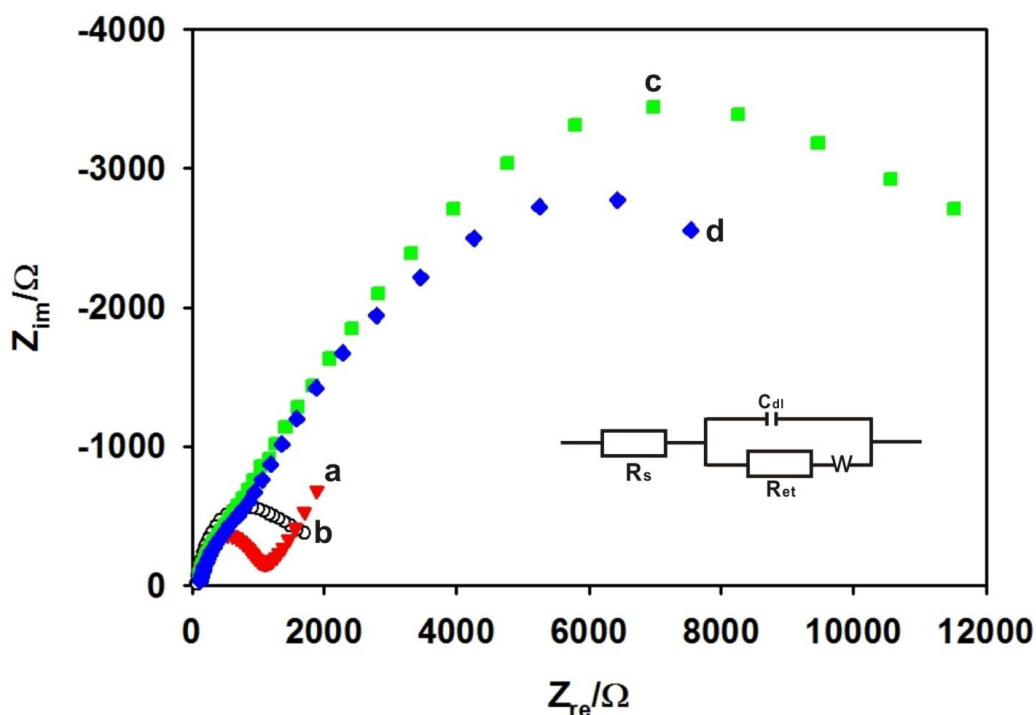


Figure 8. EIS of (a) bare/GCE, (b) CAT/GCE, (c) ERGO/GCE and (d) NF/CAT/ERGO/GCE recorded in 0.05 M PBS (pH 7) containing 5 mM $\text{Fe}(\text{CN})_6^{3-/4-}$. Amplitude: 5 mV, frequency: 100 mHz to 100 kHz. Inset is the Randles equivalence circuit used to fit the EIS data obtained at all the modified electrodes.

Fig. 8 shows the real and imaginary parts of the impedance spectra represented as Nyquist plots (Z_{im} vs. Z_{re}) for bare, CAT, ERGO and NF/CAT/ERGO/GCEs recorded in 0.05 M PBS (pH 7) containing 5 mM $\text{Fe}(\text{CN})_6^{3-/4-}$. Inset is the Randles equivalence circuit model used for fitting the EIS data of the above mentioned electrodes. From the best fitted model, we have calculated the electron transfer resistance (R_{et}) values. In Fig. 8, curve (a) represents the Nyquist plot of bare/GCE with well-defined semicircle. The R_{et} value is 950 Ω . The Nyquist plot of CAT/GCE represented by curve (b) depicts an enlarged semicircle than bare/GCE, indicating the sluggish electron transfer process. The R_{et} value observed at CAT/GCE is 1590 Ω . However, as shown in curves (c) and (d), ERGO and NF/CAT/ERGO/GCEs doesn't show well-defined semicircles in the investigated frequency range,

instead they exhibit slightly curved line validating the diffusion-limited electrochemical process. The absence of semicircle region in the Nyquist plots of ERGO and NF/CAT/ERGO films indicates the good electron transfer ability of ERGO.

3.6 Electrocatalytic H_2O_2 reduction studies

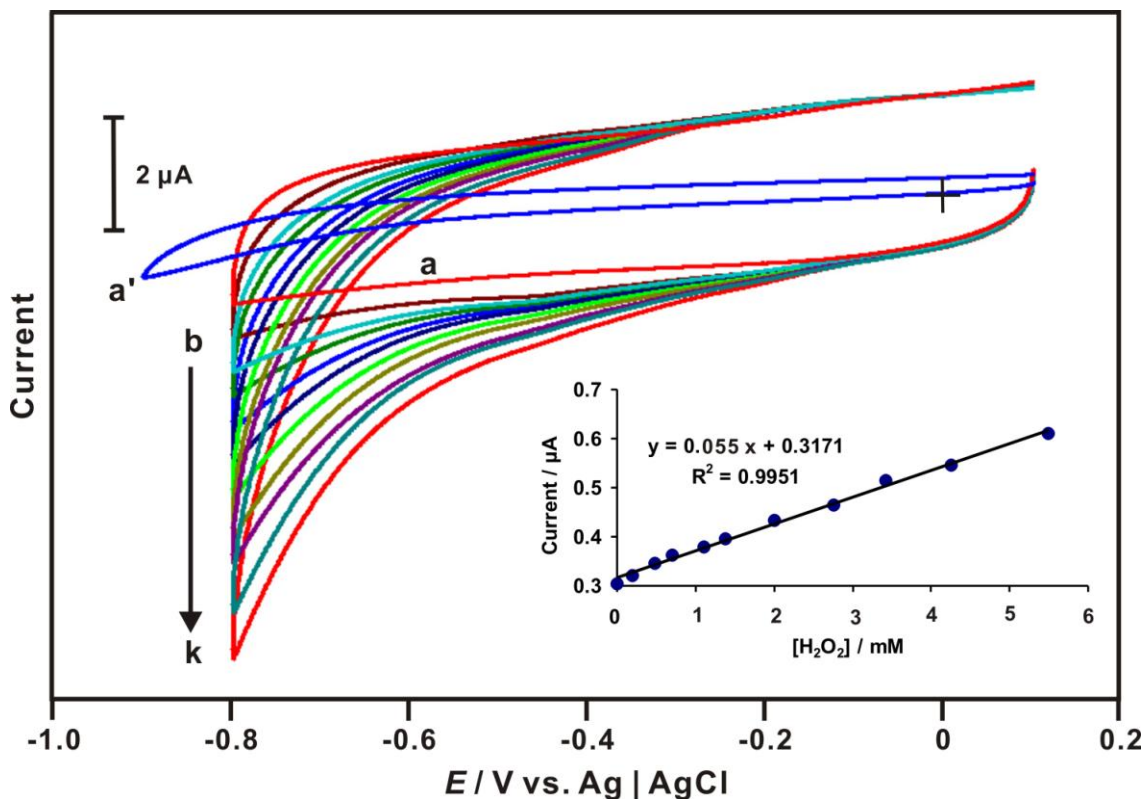


Figure 9. Cyclic voltammograms obtained at NF/CAT/ERGO/GCE at the scan rate of 50 mV s^{-1} in the a) absence and presence of (b) 0.02, (c) 0.19, (d) 0.48, (e) 0.71, (f) 1.1, (g) 1.38, (h) 2.0, (i) 2.75, (j) 3.42 and (k) 5.5 mM H_2O_2 . (a') Cyclic voltammogram obtained at bare/GCE in the presence of 5.5 mM H_2O_2 at same conditions. Supporting electrolyte is N_2 saturated 0.05 M PBS (pH 7). Inset is the plot of cathodic peak current vs. $[H_2O_2]/\text{mM}$.

Fig. 9 shows the cyclic voltammograms obtained at NF/CAT/ERGO/GCE film modified GCE in the presence of different H_2O_2 concentrations in N_2 saturated 0.05 M PBS (pH 7) at 50 mV s^{-1} scan rate. The potential range used is from 0.1 to -0.8 V. Upon the addition of 0.02 mM H_2O_2 , the electrocatalytic reduction peak current starts at -0.4 V. An enhanced reduction peak is observed at an I_{pc} of -0.6 V for 2 mM H_2O_2 . This cathodic peak current increased gradually with increase in H_2O_2 concentration additions up to 5.5 mM, while I_{pa} decreased ((Fig. 9 (b-g)). Where, both the increase in peak current and decrease in over potential are considered as electrocatalysis [16]. However, no significant catalytic peak is observed at bare GCE even in the presence of highest H_2O_2 concentration (5.5 mM) and although the potential was swept towards more negative potential of -0.9 V (Fig. 9 (a')). This result confirms that the composite film modified GCE exhibits enhanced electrocatalytic activity

towards H_2O_2 and it significantly reduces the over potential for H_2O_2 oxidation. The composite film modified GCE exhibits excellent electrocatalytic response towards H_2O_2 in the linear concentration range between 0.02 to 5.5 mM H_2O_2 with a sensitivity of $0.696 \mu\text{A mM}^{-1} \text{cm}^{-2}$ (Fig. 9 inset). The linear regression equation is $I (\mu\text{A}) = 0.055 C (\mu\text{M}) + 0.3171$, $R^2 = 0.9951$. The % relative standard deviation (R.S.D) for five successive 2 mM H_2O_2 measurements at NF/CAT/ERGO/GCE is 5.2 % which shows the acceptable repeatability of the proposed method.

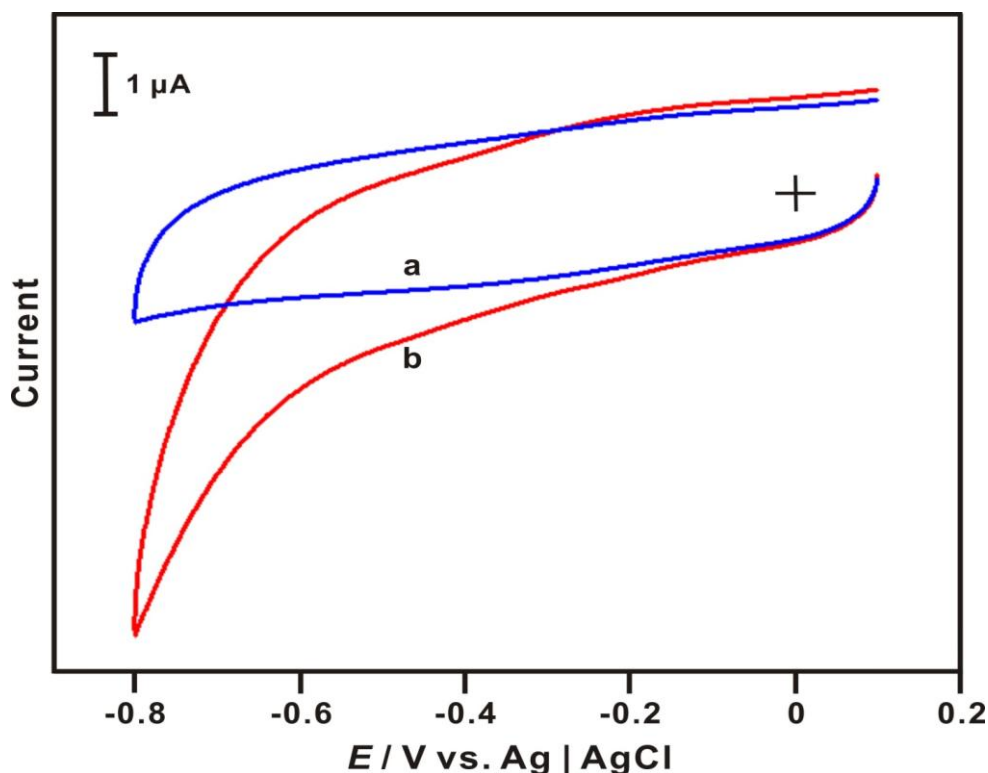


Figure 10. Cyclic voltammograms obtained at (a) NF/CAT/ERGO and (b) ERGO modified GCEs at the scan rate of 50 mV s^{-1} in the presence of 5.5 mM H_2O_2 . Supporting electrolyte is N_2 saturated 0.05 M PBS (pH 7).

In Fig. 10, curves (a) and (b) shows the cyclic voltammograms obtained at NF/CAT/ERGO and ERGO modified GCEs in the presence of 5.5 mM H_2O_2 . It is clear that the composite film shows enhanced electrocatalytic H_2O_2 reduction peak than ERGO. Thus the electrocatalytic activity of the composite film is several folds higher than the electrocatalytic activity of ERGO film. The good electrocatalytic activity of the composite film can be ascribed to the well immobilized CAT.

3.7. Amperometric H_2O_2 reduction studies

Nanomaterials incorporated enzymes based amperometric H_2O_2 biosensors have been used for achieving sensitive H_2O_2 quantification in wide linear range [17-21]. In the present study we have used amperometry technique to evaluate the performance of the developed CAT biosensor. During the

amperometric experiments the electrode potential was hold at -0.45 V and the N_2 saturated 0.05 M PBS (pH 7) was continuously stirred at 900 RPM. For every 50 s, aliquots of H_2O_2 were successively injected into the supporting electrolyte solution. Fig. 11 (A) shows the amperometric $i-t$ response obtained at NF/CAT/ERGO rotating disc GCE upon various H_2O_2 concentration additions.

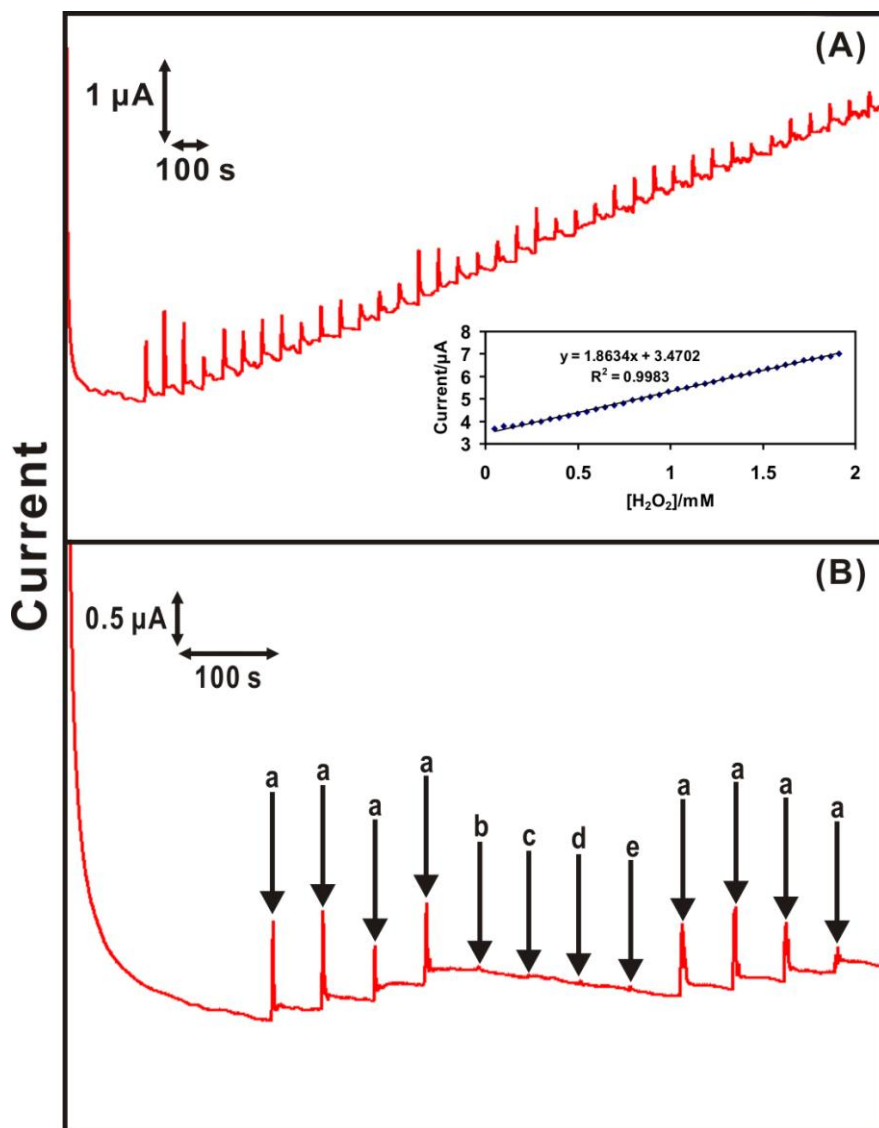


Figure 11. (A) Amperometric $i-t$ response at NF/CAT/ERGO film modified rotating disc GCE upon successive additions of 0.05 - 1.91 mM H_2O_2 into continuously stirred N_2 saturated 0.05 M PBS (pH 7). Applied potential: -0.45 V; Rotation rate: 900 RPM. Inset is the plot of response current vs. $[H_2O_2]/mM$. (B) Amperometric $i-t$ response at NF/CAT/ERGO/GCE for the successive addition of 0.05 mM H_2O_2 (a); (b) 0.05 mM AA, (c) 0.05 mM UA, (d) 0.05 mM L-cystine and (e) 0.05 mM glucose solution additions. Supporting electrolyte: continuously stirred N_2 saturated 0.05 M PBS (pH 7) solution. The other experimental conditions are same as that of Fig. 11 (A).

It is clear that, composite film exhibits rapid, well-defined amperometric response towards each H_2O_2 concentration additions. The response time of the NF/CAT/ERGO composite film towards H_2O_2 is 5 s, validating the rapid catalytic reduction process occurring at the composite film surface. The response current increases linearly between 5.09×10^{-3} M and 1.5×10^{-2} M H_2O_2 concentration additions (see Fig. 11 (A) inset). From the calibration plot, the linear concentration range, correlation coefficient and sensitivity values are calculated as 0.05-1.91 mM H_2O_2 , 0.9983 and $7.764 \mu\text{A mM}^{-1} \text{cm}^{-2}$, respectively. The linear regression equation is $I (\mu\text{A}) = 1.8634 C (\mu\text{M}) + 3.4702$, $R^2 = 0.9983$. The satisfactory amperometric H_2O_2 determination results achieved at the NF/CAT/ERGO film could be attributed to the good affinity of immobilized CAT towards H_2O_2 .

In order to determine H_2O_2 from real samples, selectivity study is mandatory for the developed CAT based biosensor. It is well known that biological fluids contain H_2O_2 along with the biomolecules like ascorbic acid (AA), uric acid (UA), L-cysteine and glucose. Therefore, selectivity of the developed NF/CAT/ERGO composite film was evaluated in the presence of above said interfering species. The technique utilized for the selectivity study was amperometric i-t curve. In Fig. 11 (B), (a) shows the rapid, well defined amperometric responses obtained at NF/CAT/ERGO composite film for 0.05 mM H_2O_2 concentration additions. However, no notable amperometric response was observed when each 0.05 mM of AA, UA, L-cysteine and glucose solutions were successively injected into the same supporting electrolyte solution (see (b-e) in Fig.11 (B)). But, well defined amperometric responses were observed immediately when each 0.05 mM H_2O_2 was injected successively into the same supporting electrolyte solution. The selectivity results thus confirmed that proposed CAT biosensor is highly selective and it successfully overcomes the matrix effect caused by the common interferences, so it could be employed for the determination of H_2O_2 from real samples.

3.8. Operational stability study

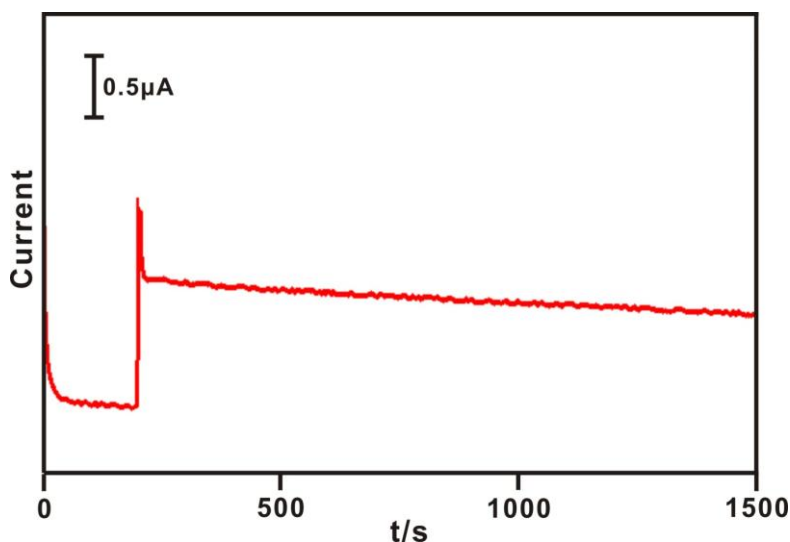


Figure 12. Amperometric i-t response at NF/CAT/ERGO film modified rotating disc GCE upon 0.05 mM H_2O_2 addition into continuously stirred N_2 saturated 0.05 M PBS (pH 7). The modified electrode was continuously rotated up to 1500s. Applied potential: -0.45 V; Rotation rate: 900 RPM.

The operational stability of NF/CAT/ERGO composite film modified rotating disc GCE was examined by amperometry. Fig. 12 shows the well-defined amperometric *i-t* response observed at NF/CAT/ERGO film modified rotating disc GCE upon the addition of 0.05 mM H₂O₂ into continuously stirred N₂ saturated 0.05 M PBS (pH 7). The response current was stable up to 1500s, which indicates the excellent operational stability of the composite film.

3.9. Real sample analysis

The practical applicability of NF/CAT/ERGO film was investigated through real sample analysis. The technique used was amperometric *i-t* curve study. Commercially available contact lens cleaning solution was purchased from a local drug store in Taipei, Taiwan. The labeled composition of H₂O₂ present in the contact lens solution is 3 %. Further dilutions were made using 0.05 M PBS (pH 7). During the amperometric experiments the working electrode potential was hold at -0.45 V. As shown in Fig. 13, NF/CAT/ERGO film modified rotating disc GCE shows excellent amperometric *i-t* response for the successive addition of H₂O₂ containing contact lens cleaning solution.

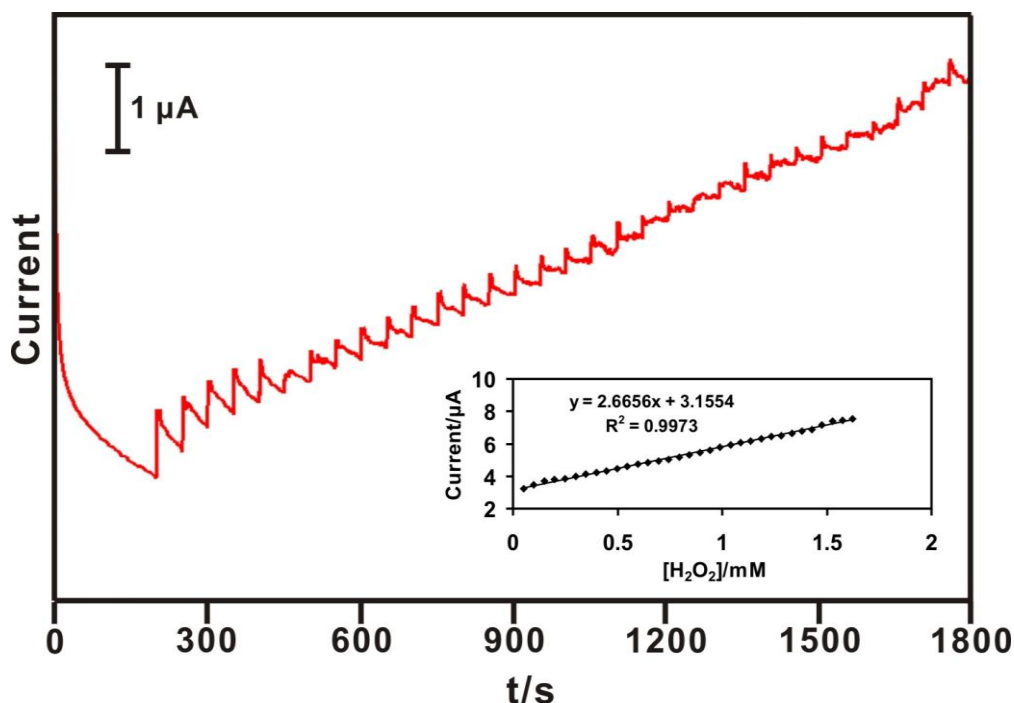


Figure 13. Amperometric *i-t* response at NF/CAT/ERGO film modified rotating disc GCE upon successive additions of 0.05-1.91 mM H₂O₂ containing contact lens cleaning solution into continuously stirred N₂ saturated 0.05 M PBS (pH 7). Applied potential: -0.45 V; Rotation rate: 900 RPM. The inset is the plot of response current vs. [H₂O₂]/mM.

For every 50 s, aliquots of H₂O₂ concentration were injected into the continuously stirring 0.05 M PBS (pH 7). The linear concentration range is between 0.05 -1.91 mM. The determination of H₂O₂

from commercially available contact lens cleaning solution in good linear range shows the good practical applicability of the composite film towards H₂O₂ determination.

4. CONCLUSIONS

We report a simple fabrication method for the development of NF/CAT/ERGO film based H₂O₂ biosensor. The direct electrochemistry of the model enzyme, CAT has been reported at ERGO modified surface in this study. The CAT immobilized ERGO sensing platform exhibits excellent electrocatalytic response towards H₂O₂ in wide range with good sensitivity. The large surface area of ERGO offers efficient enzyme loading and it facilitates fast electron transfer kinetics. The NF outer protective layer adds good stability to the biosensor and as a result it shows remarkable operational stability. Moreover, the proposed biosensor shows excellent selectivity and it detects H₂O₂ from contact lens solution in good linear range.

ACKNOWLEDGEMENT

This work was supported by the National Science Council and the Ministry of Education of Taiwan (Republic of China).

References

1. Y. Zhu, S. Murali, W. Cai, X. Li, J.W. Suk, J.R. Potts, R.S. Ruof, *Adv. Mater.*, 22(2010) 3906.
2. Y. Shao, J. Wang, H. Wu, J. Liu, I.A. Aksay, Y. Lin, *Electroanal.*, 22 (2010) 1027.
3. M. Inagaki, Y.A. Kim, M. Endo, *J. Mater. Chem.*, 21 (2011) 3280.
4. R.Y.N. Gengler, A. Veligura, A. Enotiadis, E.K. Diamanti, D. Gournis, C. Jozsa, B.J.V. Wees, P. Rudolf, *Small*, 6 (2010) 35.
5. J. Shen, Y. Hu, M. Shi, X. Lu, C. Qin, C. Li, M. Ye, *Chem. Mater.*, 21 (2009) 3514.
6. H.L. Guo, X.F. Wang, Q.Y. Qian, F.B. Wang, X.H. Xia, *Nano lett.*, 3 (2009) 2653.
7. X. Dong, W. Huang, P. Chen, *Nanoscale. Res. Lett.*, 6 (2011) 60.
8. P.A. Prakash, U. Yogeswaran, S.M. Chen, *Talanta*, 78 (2009) 1414.
9. P.A. Prakash, U. Yogeswaran, S.M. Chen, *Sensors*, 9 (2009) 1821.
10. A. Salimi, E. Sharifi, A. Noorbakhsh, S. Soltanian, *Biophys. Chem.*, 125(2007) 540.
11. B. Zhou, J. Wang, X. Gao, Y. Tian, *Anal. Lett.*, 41(2008) 1832.
12. L. Shen, N. Hu, *Biomacromolecules*, 6 (2005) 1475.
13. K.J. Huang, .D.J. Niu, X. Liu, Z.W. Wu, Y. Fan, Y.F. Chang, Y.Y. Wu, *Electrochim. Acta*, 56 (2011) 2947.
14. L. Staudenmaier, *Ber. Dtsch. Chem. Ges.*, 31 (1898) 1481.
15. R. Muszynski, B. Seger, P.V. Kamat, *J. Phys. Chem. C*, 112 (2008) 5263.
16. C.P. Andrieux, O. Haas, J.M. Savgant, *J. Am. Chem. Soc.*, 108 (1986) 8175.
17. J. S. Xu, G.C. Zhao, *Int. J. Electrochem. Sci.*, 3 (2008) 519.
18. L. Zhang, Z. Fang, Y. Ni, G. Zhao, *Int. J. Electrochem. Sci.*, 4 (2009) 407.
19. L.S. Duan, Q. Xu, F. Xie, S.F. Wang, *Int. J. Electrochem. Sci.*, 3 (2008) 118.
20. A.K. Upadhyay, Y.Y. Peng, S. M. Chen, *Sens. Actuators, B*, 141 (2009) 557.
21. A. P. Periasamy, S. W. Ting, S.M. Chen, *Int. J. Electrochem. Sci.*, 6 (2011) 2688.